IUST
Iran University of Science and Technology

Iranian Journal of Electrical and Electronic Engineering

Journal Homepage: ijeee.iust.ac.ir

Modified Richardson-Lucy Deconvolution Algorithm for Image Restoration

Jaliba Sherin *, Shajee Mohan B S **(C.A.) and Ahammed Muneer K V ***

Abstract: Effective image processing involves image restoration as a major task. When image is being acquired or being sent, they frequently suffer from degradation. Blurring, data loss as a result of sampling, quantization effects, and other noise sources are all examples of degradation. Trying to recreate or prepare an estimate of the original image from a degraded image is the goal of image restoration. For image restoration from degraded and damaged images, the Richardson-Lucy deconvolution technique is frequently used. We suggest a modified version of the original Richardson-Lucy deconvolution technique in this paper, to find the best deconvolution transfer function. We also propose a method to obtain the optimal deconvolution transfer function in a class-specific way. We considered performance metrics such as PSNR, MSE, SSIM and KL Divergence for evaluating the performance of the proposed restoration processes and evaluated the performances of different implementations of the Richardson-Lucy deconvolution algorithm. It is seen that the results are at par and in some cases superior to the existing techniques. A close examination of the proposed methodology, it is seen that the proposed class-specific Richardson-Lucy deconvolution method outperforms all other techniques.

Keywords: Richardson-Lucy deconvolution algorithm, Optimal transfer function, Support Vector Machine, MSE, KL Divergence, SSIM, PSNR

1 Introduction

DURING the data acquisition or in the transmission process, the images are degraded. Image restoration is typically employed in a variety of fields of image processing and applications that include areas such as forensic research, remote sensing, microscope imaging, medical imaging, and astronomical imaging.

The quality of images is very badly degraded in numerous circumstances such as imaging that involves motion, blur conditions that involve sensing through a diffusing medium, and low signal-to-noise conditions. Getting the original image from a hazy image, degraded astronomical image, images that are taken during rain, and also from underwater is challenging. In this paper, we are trying to acquire an estimate of the original image by creating a reconstruction model. Assuming some understanding of the degradation phenomenon, restoration of an image is the process of recovering from its deteriorated version. To get the original image from the deteriorated (observed) image, the degradation process is modelled and then reversed. In contrast to picture enhancement, image restoration that does not fully account for the nature of the degradation. Restoration of image is performed with the aid of restoring the image information lost as a result of the blurring process, is done by making use of a point source, known as the Point Spread Function (PSF). This reverses the process that caused the image to become blurry.

Iranian Journal of Electrical & Electronic Engineering, 2027.
Paper first received 24 August 2025 and accepted 12 August 2026.
* The author is with the Department of M.Tech Signal Processing, AE&I, Govt. Engineering College Kozhikode, Kerala, India.
** The author is with the Department of CSE, SSCSE, Sharda University, Greater Noida, UP, India.
*** The author is with the Department of AE&I, GEC, Engineering College Kozhikode, Kerala, India.
E-mails: shajee.mohan@sharda.ac.in.
Corresponding Author: Shajee Mohan B S.

In Press

2 REVIEW OF LITERATURE

There are several existing techniques that yield image restoration such as based on ICA [1], [3], [11], phase field modal [2], Adaptive quantile sparse image [4], Alternative feature refinement network [5], Deep learning [6], Wiener filter [8], non-local variational technique based on structural similarity index [7], Blind deconvolution [9] and inverse filtering [12].

Mingli Zhang et al., [10] proposed a new image restoration technique that merges non-local self-similarity and global structure sparsity for the restoration of high-quality images. Utilizing a weighted nuclear norm-based adaptive regularization technique, bunches of identical patches were simultaneously reconstituted. The global structure is kept by the use of a creative approach. The image is split into a sparse residual and a smooth component. L1 norm was used to regularize the latter. Images that have been corrupted are recovered using a strategy for optimization grounded in the Alternating Direction Method of Multipliers (ADMM) algorithm. The performance is evaluated based on image completion and super-resolution. José M. Bioucas-Dias et al., [13] proposed a method to handle unconstrained optimization problems seen in image restoration. This type of problem comes from the combination of a linear observation model and a non-quadratic regularizer.

Bonmassar et al., [14] proposed a system that restores the real-time image which is degraded by uniform motion blur in the foveal active vision system. Yong Chen et al., [15] proposed a collection of sparsity regularization methods for the spatial difference images in HSI restoration. A series of experimental findings using both simulated and original data serve to illustrate HSI restoration. Jose A. Guerrero-Colón et al., [16] proposed an enhancement technique to approximate the local signal covariance, a model with a coarser adaption level is introduced in each sub-band.

A photoacoustic tomography image restoration with measured spatially variant PSF was discussed in [17]. The iterative restoration model shown significant image quality. Unsupervised image restoration with quality-task-perception loss was described in [18]. The experiments on three datasets shown superior performance. An image restoration method with generalized image formation model for poor visible conditions was discussed in [19]. Experiments suggested that the GIFM performs well for image restoration of extreme scenes, keypoint detection, object detection, and image segmentation. Local adaptive prior-based image restoration method for space diffraction imaging systems was discussed in [20]. A blind JPEG restoration strategy called DriftRec was discussed in [21]. It has been experimentally established that DriftRec naturally generalizes to realistic and difficult scenarios such as unaligned double JPEG compression and blind restoration of JPEGs found online, without having encountered such examples during training. An extensive survey and future trends in image restoration is discussed in [22]. Modern approaches for image restoration using deep learning, extracting accurate information using frequency selection methods and visual clarity enhancement are discussed in [23-25]. A novel technique for image restoration from motion blurred images using Richardson-lucy technique is explored in [26].

In this paper, we propose a system that makes use of a modified Richardson-Lucy deconvolution algorithm to recover the estimate of original images. We analyzed the performance of the various techniques using performance metrics such as Peak Signal to Noise Ratio (PSNR), Mean Square Error (MSE), SSIM (Structural Similarity Index Measure), and Kullback-Leibler Divergence (KLD). In this work, we experimented with three different techniques, the Richardson-Lucy deconvolution algorithm is used to reconstruct the original image. We used a dataset that consists of five different classes from the Caltech 101 benchmark dataset, and we also created a custom Dataset-2 that includes popular benchmark single images. A concise description of the novel aspects introduced to the Richardson–Lucy deconvolution algorithm and the primary contributions of the suggested work are outlined below:

- We implemented a standard Richardson-Lucy deconvolution algorithm and determined a single optimum transfer function.
- We executed a modified Richardson-Lucy deconvolution algorithm with an iterative procedure to determine the optimum transfer function for deconvolution.
- Developed a class-specific Richardson-Lucy deconvolution algorithm. In this modified method we introduced a technique to iteratively determine the optimal deconvolution transfer function in a class-specific way. In this method, we obtain five different optimal deconvolution transfer functions for five different classes.

The remaining part of the paper is organized as follows: Section 3 describes the experimental details and methodology followed in this work for image restoration. Various results and analyses are given in Section 4. Finally, we conclude the study in Section 5.

3 EXPERIMENTAL DETAILS

In the proposed method, we initially added distinct kinds of noises such as Gaussian noise, motion blur, salt

In Press

and pepper noise, speckle noise, local variance, Poisson noises, erosion, dilation, etc., to prepare a set of degraded images from a set of original images. The dataset split in to a training and test set of images. For image restoration, we need PSF i.e., the optimal transfer function for deconvolution. In this work, we implemented three methods for image restoration using variants of Richardson–Lucy deconvolution techniques.

3.1 Richardson-Lucy Deconvolution

An iterative process called the Richardson-Lucy deconvolution algorithm is used to recover an underlying image that has been obscured by a recognized PSF.

When an optical system generates an image and it is captured, for example, by photographic film or a charge-coupled device, an ideal point source does not manifest as a point but is instead spread across the PSF. Since extended sources can be represented as the sum of several individual point sources, the resulting image can be described using a transition matrix P applied to a fundamental image:

$$d_i = \sum_j P_{i,j} u_j \tag{1}$$

Where u_j is the underlying image's pixel-level brightness at j the pixel. Here d_i is the ith pixel's observed intensity. Typically, a matrix whose elements are $P_{i,j}$ describes the amount of light detected in pixel i from source pixel j. The transfer function P in the majority of the spatial offset between the source pixel j and the observation pixel i in excellent optical systems (or generically in linear systems defined as shift invariant) can be represented as follows:

$$P_{i,j} = P(i - j) \tag{2}$$

where $P(\Delta i)$ is called a one-dimensional PSF. The aforementioned equation then turns into a convolution. For a 2-D imaging system we consider $P(\Delta x, \Delta y)$, a 2-D point spread function. For obtaining an estimation of u_j , for a given the observed d_i , and the known $P(\Delta i_x, \Delta j_y)$ We use the following iterative process, to compute update $\hat{u}_j^{(t+1)}$ from $\hat{u}_j^{(t)}$. Where $\hat{u}_j^{(t)}$ is an estimate of u_j at time t.

$$\hat{u}^{(t+1)} = \hat{u}_j^{(t)} \sum_i \frac{d_i}{c_i} p_{i,j} \tag{3}$$

where,

$$c_i = \sum_j p_{ij}\, \hat{u}_j^{(t)} \tag{4}$$

Empirical evidence suggests that if this iteration converges, it will achieve this with the most probable solution for u_j. Writing this in terms of convolution with a PSF more generally P for two (or more) dimensions:

$$\hat{u}^{(t+1)} = \hat{u}^{(t)} \cdot \left(\frac{d}{\hat{u}^{(t)} \otimes P} \otimes P^* \right) \tag{5}$$

Where, $\otimes$ represents a 2D convolution, and P^* is the mirrored PSF. When there are issues, the PSF $p_{i,j}$ is known a priori. Blind deconvolution can be achieved by modifying the Richardson-Lucy algorithm to account for information that cannot be predicted beforehand.

3.2 DATASET

We use five different classes of images from the Caltech 101 benchmark dataset that include Butterfly, Couger, Faces, Pizza, and Sunflower (Caltech 101-5). We also use a custom dataset that consists of single images that includes popular benchmark images such as Cameraman, Lena, Barbara, Baboon, and Devi, etc. (Dataset-2).

3.3 Degradation of images

In order to degrade the image, we added different types of noises. While adding Gaussian noise to the image, we vary the value of standard deviation (σ), to obtain different grades of influence of noise. The original image is blurry even after adding motion blur. If the value of σ increases, the impact of motion blur also increases. Considering the image which is degraded by speckle noise, when the σ value increases the speckle in the image also increases. While adding local variance to the original image, the quality of the image decreases to σ value increases. Degradation is high when σ value is high. Image quality is greatly affected by Gaussian noise, motion blur, speckle noise, and local variance. Based on the value of σ, the level of degradation present in an image varies.

The representative images showing the effect of adding different noises are depicted in Fig.1 to Fig.3.



(a) Original Image (b) Added Gaussian noise

Fig 1. Original Image is added with Gaussian noise.

In Fig.1, the original image is added with Gaussian noise. Motion blur has been added to the original image, as seen in Fig. 2. The initial image in Fig. 3 is given a sequence of noise. From the degraded image, we learn the

In Press

model parameters. Using the learned parameter and degraded test image, we restored the estimate of the original image. Finally, we analyze the performance metrics.



(a) Original Image (b) Added motion blur

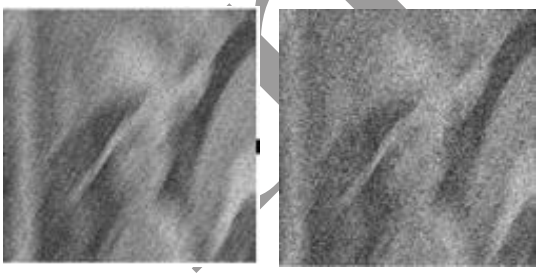
Fig 2. Original Image is added with Motion blur.



(a) Original Image (b) Added Gaussian noise



(c) Added motion blur



(d) Added Salt and pepper (e) Added Local variance

Fig 3. Original image is added with Gaussian, Motion blur, Salt and pepper, and Local variance in a sequential way.

3.4 Image Restoration

3.4.1. Standard Richardson-Lucy Deconvolution Algorithm

To have a baseline for performance comparison, we try to restore the image by using the standard Richardson-Lucy deconvolution algorithm. Training images are degraded by blur, Gaussian noise, etc. We use a test image, that is degraded randomly, and obtain the estimate of the original image using the standard Richardson-Lucy deconvolution algorithm. We evaluated the performance metrics such as MSE, PSNR, SSIM, and KLD and tabulated the values.

3.4.2. Modified Richardson-Lucy deconvolution algorithm with an iterative procedure

To The modified Richardson-Lucy deconvolution algorithm consists of an iterative procedure. Training images are degraded and restored by selecting a random transfer function and corresponding performance metrics are noted. In each iteration step, we consider MSE as the performance criterion for comparison. The transfer function that is used for image restoration is stored in an array and the corresponding MSE value is also kept in the array. For each image, we consider a maximum of a hundred iterations. Finally, we observe the least MSE value from that array, and the corresponding transfer function is selected and stored.

This transfer function is the optimal transfer function of a single image and in the same way, we find the optimal transfer function for all images. After finding the transfer function for every image in the training dataset, we take the average of all the transfer functions. That average value is considered the optimal transfer function for deconvolution of degraded images. Here we have only a single transfer function to regain the original image. We tabulated the values of performance metrics in Tables 4 and 5.

3.4.3. Class-specific modified Richardson-Lucy deconvolution algorithm

In this method, to discover the best deconvolution transfer function in a class-specific manner, we introduce a modified Richardson-Lucy deconvolution technique with an iterative process. We used the Caltech 105-5 dataset. Training images of each class are degraded and restored by selecting a random transfer function and corresponding performance metrics are noted. Here we consider MSE for performance comparison. The transfer function which is used for image restoration is stored in an array and the corresponding MSE value is also stored in the array. Finally, we observe the least MSE value from that array, and corresponding transfer functions are selected and stored in a separate array.

This transfer function is the optimal transfer function of a single image and in the same way, we find optimal transfer functions for all images in a class. After finding the transfer functions for every image in the training set of each class, we accept the average of that transfer function. That average value is considered the optimal transfer

In Press

function for deconvolution of degraded images for that class. Here we have five different transfer functions for five different classes. A degraded image is given to the SVM classifier to obtain the class label of the degraded image. Then we use the corresponding optimal transfer function specific to that class for the class-specific Richardson-Lucy deconvolution algorithm. It is seen that the image fis restored with better performance metrics.

3.5 Performance Metrics

3.5.1. Peak Signal-to-Noise Ratio (PSNR)

The PSNR ratio measures the strength of corrupting noise to the highest attainable power of an image.

$$\mathrm{PSNR} = 20\log_{10}\left(\mathrm{MAX}/(\mathrm{MSE})^{(1/2)}\right) \tag{6}$$

$$\mathrm{MAX} = \mathrm{L} - 1 \tag{7}$$

where L is the maximum pixel value. where $\mathrm{L} = 2^{\mathrm{B}}$ and B= 8-bit.

$$\mathrm{MSE} = \frac{1}{\mathrm{kl}}\sum_{\mathrm{m}=0}^{\mathrm{k}-1}.\sum_{\mathrm{n}=0}^{\mathrm{l}-1}\left(\mathrm{O}(\mathrm{m},\mathrm{n}) - \mathrm{R}(\mathrm{m},\mathrm{n})\right)^2 \tag{8}$$

3.5.2. Structural Similarity Index Measure (SSIM)

SSIM is a measuring tool for finding the discerning quality in several digital videos together with images. The SSIM index can be determined on different image windows. Let us consider two windows i and j with usual size N × N and SSIM is:

$$(\mathrm{i},\mathrm{j}) = \frac{\left(2\mu_{\mathrm{i}}\mu_{\mathrm{j}} + \mathrm{C}_1\right)\left(2\sigma_{\mathrm{ij}} + \mathrm{C}_2\right)}{\left(\mu_{\mathrm{i}}^2 + \mu_{\mathrm{j}}^2 + \mathrm{C}_1\right)\left(\sigma_{\mathrm{i}}^2 + \sigma_{\mathrm{j}}^2 + \mathrm{C}_2\right)} \tag{9}$$

μ_{i} the mean of the image i.

μ_{j} the mean of the image j.

σ_{i}^2 the standard deviation of the image i.

σ_{j}^2 the standard deviation of the image j.

σ_{ij} the covariance of the image i and image j.

$\mathrm{C}_1 = (\mathrm{k}_1\mathrm{L})^2$, $\mathrm{C}_2 = (\mathrm{k}_2\mathrm{L})^2$ is a variable to maintain balance during division when the numerator is zero. L is the dynamic range of pixel values, $\mathrm{k}_1 = 0.01$ and $\mathrm{k}_2 = 0.03$.

3.5.3. KL Divergence (Kullback-Leibler divergence)

It serves as a gauge of statistical separation. KL Divergence measures how two reference probability distributions P and Q diverge from each other. KL divergence from Q to P is given by:

$$\mathrm{D}_{\mathrm{KL}}(\mathrm{P}\,||\mathrm{Q}) = \sum_{\mathrm{x}\in\mathrm{x}} \mathrm{P}(\mathrm{x})\log\frac{\mathrm{P}(\mathrm{x})}{\mathrm{Q}(\mathrm{x})} \tag{10}$$

The KL divergence score, also known as the Kullback-Leibler Divergence score, estimates how one probability distribution differs from a second probability distribution. Let Q and P are two probability distribution.

The KL divergence can be expressed by employing the notation KL (P || Q), where the operator || shows "divergence" or the divergence of P and Q. The log of the probability of the event in Q over the probability of the event in P can be used to calculate the KL divergence, which is the negative sum of the probabilities of each event in P.

3.5.4. Mean Square Error (MSE)

MSE represents the total squared error between the original image and the restored one. It assesses the similarity between the reconstructed image and the original image.

$$\mathrm{MSE} = \frac{1}{\mathrm{kl}}\sum_{\mathrm{m}=0}^{\mathrm{k}-1}.\sum_{\mathrm{n}=0}^{\mathrm{l}-1}\left(\mathrm{O}(\mathrm{m},\mathrm{n}) - \mathrm{R}(\mathrm{m},\mathrm{n})\right)^2 \tag{11}$$

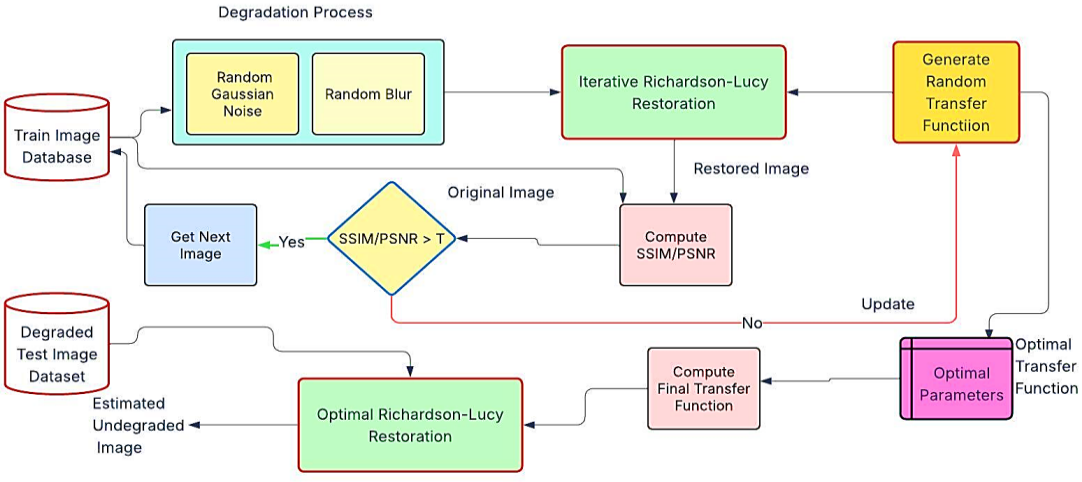


Fig 4. Block diagram of modified Richardson-Lucy deconvolution method.

In Press

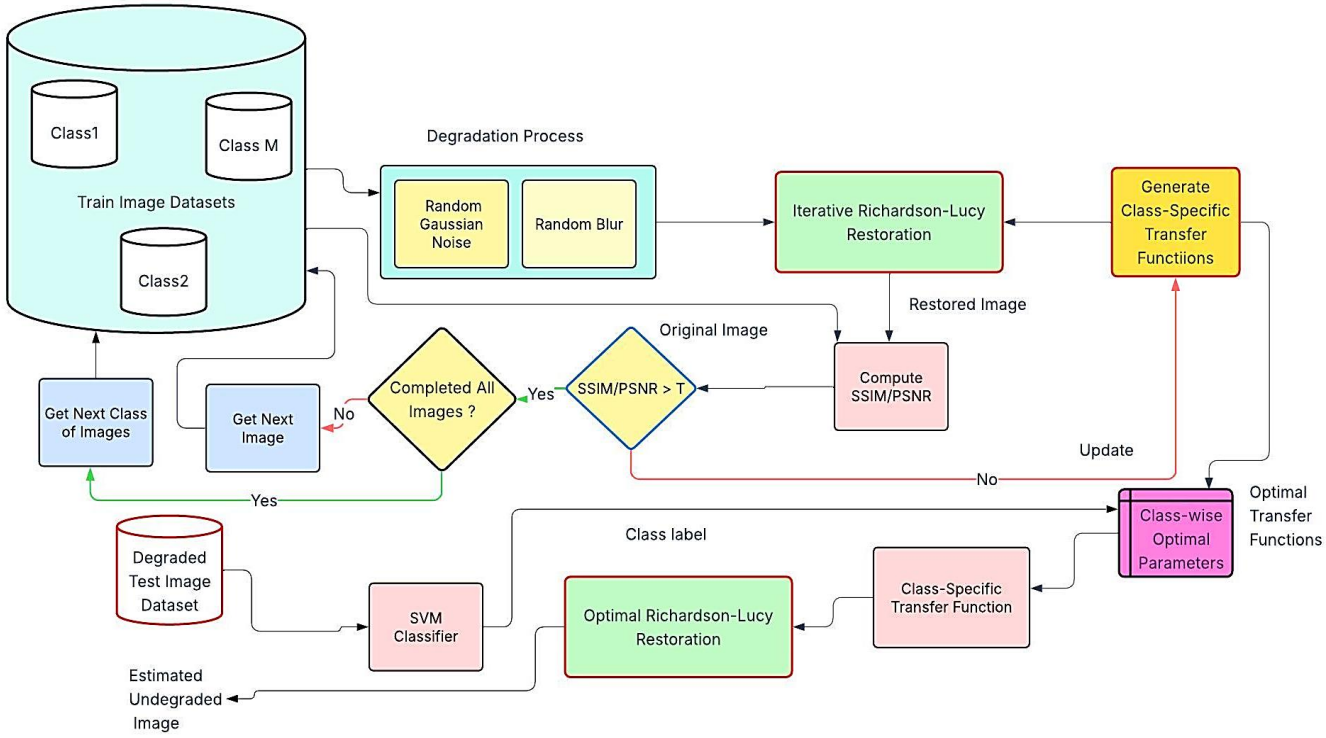


Fig 5. Block diagram of Modified Richardson-Lucy Deconvolution Method.

Table 1. Description datasets used in the experiments.

Dataset	No. of Training Images	No. of Test Images	Size (pixel × pixel)
Butterfly	82	10	512× 512
Cougar	60	9	512× 512
Faces	392	43	512× 512
Pizza	48	5	512× 512
Sunflower	75	10	512× 512
Dataset-2	Single image	Single image	512× 512

4 RESULTS AND DISCUSSION

In this paper we considered performing image restoration using standard, modified, class-specific Richardson-Lucy deconvolution algorithms. The observations and findings are discussed below:

4.1 Standard Richardson-Lucy Deconvolution algorithm

Recovered the image using the standard Richardson-Lucy Deconvolution algorithm. Performance metrics are analyzed for Caltech 101-5 and Dataset-2.

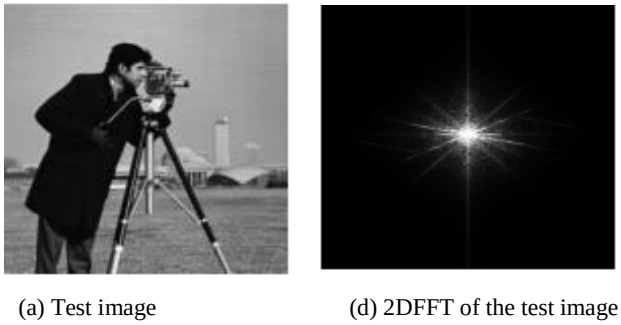
The representative test, degraded and restored images, and their corresponding 2DFFT are shown in Fig.6. Also we determined the performance metrics for the Caltech 101-5 dataset and Dataset-2. Here we considered the test images from each class as indicated in Table 1, for images Butterfly, Cougar, Faces, Pizza, and Sunflower respectively. The custom Dataset-2 includes single images named Cameraman, Lena, Baboon, Barbera, and Devi respectively. We analyzed the PSNR of the original image and degraded image (B-O), PSNR of the original image and restored image (R-O), SSIM, MSE, and KL divergence values are tabulated in Table 2 and Table 3. We considered 95% confidence level and the values given in the Table 2, Table 4 and Table 6 shows the average values and margin of error in the confidence interval.

4.2 Modified Richardson-Lucy Deconvolution Algorithm

Recovered the image using a modified Richardson-Lucy Deconvolution algorithm with an iterative procedure. In this method, we obtain a single optimal transfer function for deconvolution.

In Pr

Performance metrics are analyzed for the Caltech 101-5 dataset and Dataset-2 and the observations are given in Table 4 and Table 5. The representative test, degraded and restored images and their corresponding 2DFFT are shown in Fig.8.



(a) Test image (d) 2DFFT of the test image

(b) Degraded image (e) 2DFFT of Degraded image

(c) Restored image (f) 2DFFT of Restored image

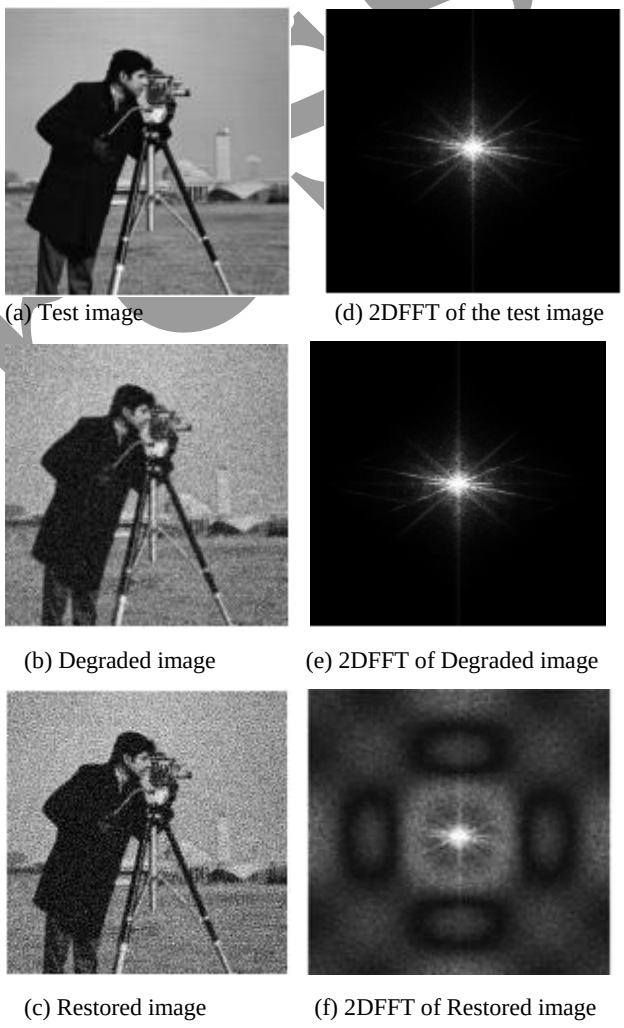
Fig 6. Representative test degraded and restored images and their corresponding 2DFFT for the Standard Richardson-Lucy deconvolution method.

Table 2. Results of standard Richardson-Lucy Deconvolution for Caltech 101-5 dataset.

Image Name	PSNR (R-O)	PSNR (B-O)	MSE	SSIM	KLD
Sunflower	15.81±0.78	14.65±1.2	0.03±.001	0.29±.01	2.63±.41
Pizza	14.45±1.02	13.39±1.4	0.05±.003	0.27±.09	2.05±.77
Faces	14.22±0.65	11.74±2.3	0.07±0.0	0.15±.04	2.20±.21
Cougar	13.47±0.68	12.50±1.4	0.06±.001	0.30±.08	3.20±.74
Butterfly	16.11±1.14	14.28±1.4	0.04±.003	0.23±.11	2.56±.64

Table 3. Results of standard Richardson-Lucy Deconvolution for Dataset-2.

Image Name	PSNR (R-O)	PSNR (B-O)	MSE	SSIM	KLD
Cameraman	17.2588	15.1303	0.0307	0.1281	2.3007
Baboon	17.5701	16.6698	0.0215	0.1691	0.9915
Barbera	18.4404	17.0656	0.0197	0.1822	0.8702
Lena	16.9175	14.7804	0.0333	0.1222	1.3663
Devi	20.0812	17.8057	0.0166	0.2183	1.7478



(a) Test image (d) 2DFFT of the test image

(b) Degraded image (e) 2DFFT of Degraded image

(c) Restored image (f) 2DFFT of Restored image

Fig 7. Representative test degraded and restored images and their corresponding 2DFFT for the Standard Richardson-Lucy deconvolution method.

4.3 Class-specific modified Richardson-Lucy deconvolution algorithm

In this study, we performed experiments to restore the original image by employing a modified class-specific Richardson-Lucy Deconvolution algorithm with an

In Press

iterative procedure. In this method, we obtain five different optimal transfer functions for different classes of deconvolution for Caltech 101-5. Performance metrics are analyzed for the Caltech 101-5 dataset and for different images in Dataset-2 with image specific transfer functions. The observations are given in Table 6 and Table 7.

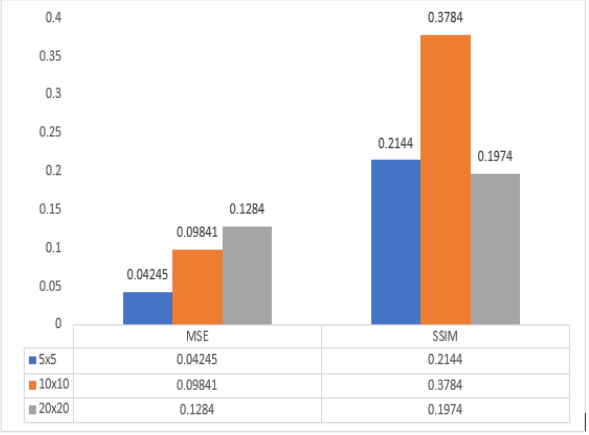


Fig 8. Graphical representation of performance metrics of the modified Richardson-Lucy deconvolution.

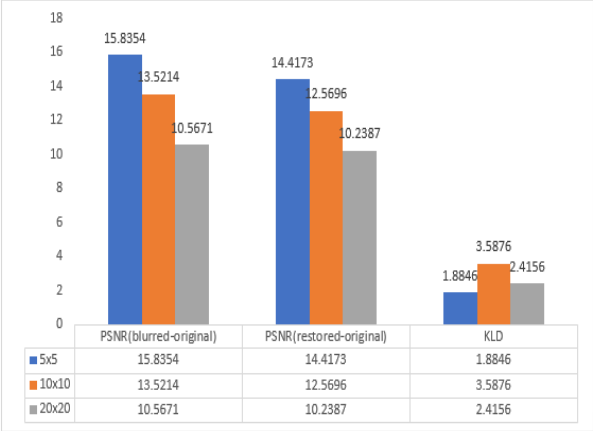


Fig 9. Graphical representation of performance metrics of the modified Richardson-Lucy deconvolution.

Table 4. Results of Modified Richardson-Lucy Deconvolution for Caltech 101-5 dataset.

Image Name	PSNR (R-O)	PSNR (B-O)	MSE	SSIM	KLD
Sunflower	14.72±0.20	12.25±0.31	0.06±0.0	0.41±0.0	2.52±.003
Pizza	15.04±2.18	14.33±2.18	0.04±0.0	0.3±0.07	1.53±0.04
Faces	13.86±1.24	11.47±1.43	0.07±0.0	0.14±0.07	2.14±0.04
Cougar	15.74±0.72	16.09±1.40	0.02±.002	0.43±0.09	2.51±0.79
Butterfly	17.36±0.20	15.77±0.31	0.03±0.00	0.27±.001	2.42±.004

Table 5. Results of Modified Richardson-Lucy Deconvolution for Dataset-2.

Image Name	PSNR (R-O)	PSNR (B-O)	MSE	SSIM	KLD
Cameraman	20.0137	18.2234	0.0151	0.1955	2.1404
Baboon	12.7725	10.7920	0.0833	0.0650	2.3320
Barbera	18.4589	17.1550	0.0193	0.1824	0.9888
Lena	18.0300	16.0798	0.0247	0.1480	-
Devi	14.4087	11.9734	0.0635	0.0785	1.8047

Table 6. Results of class-specific Richardson-Lucy Deconvolution for Caltech 101-5 dataset.

Image Name	PSNR (R-O)	PSNR (B-O)	MSE	SSIM	KLD
Sunflower	20.86±0.2	20.86±0.31	0.008±0	0.67±0.0	0.29±.003
Pizza	14.12±2.18	14.12±2.18	0.04±0.0	0.50±.07	0.74±0.04
Faces	18.59±1.24	18.14±1.4	0.01±0.0	0.32±.06	3.22±0.04
Cougar	16.6±0.68	16.6±1.4	0.02±.0.0	0.19±.08	0.79±.74
Butterfly	8.94±1.79	8.94±1.9	0.13±0.0	0.05±0.7	1.6±0.04

Table 7. Results of class-specific Richardson-Lucy Deconvolution for Dataset-2.

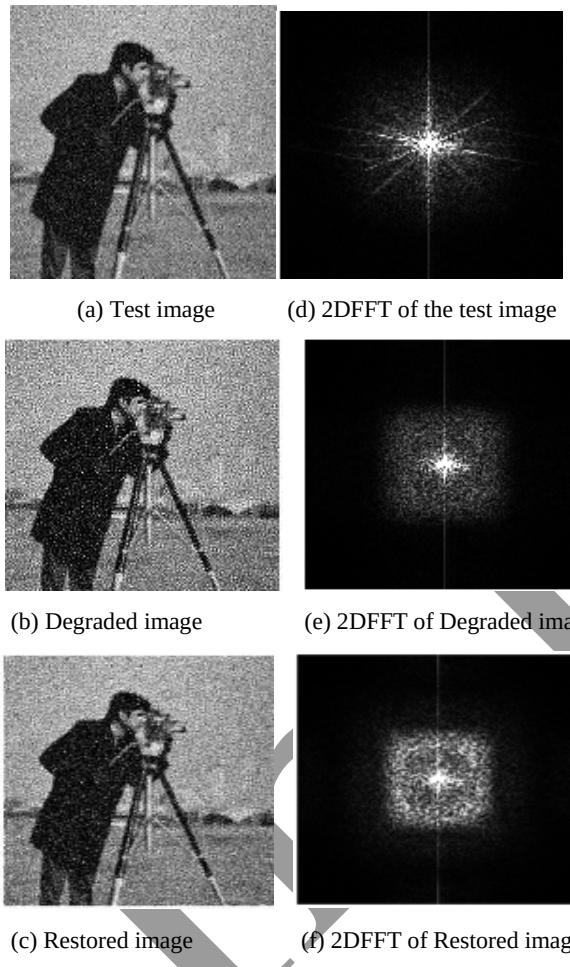
Image Name	PSNR (R-O)	PSNR (B-O)	MSE	SSIM	KLD
Cameraman	15.9930	15.1303	0.0252	0.2367	1.3427
Baboon	13.5358	13.5358	0.0443	0.1563	0.8796
Barbera	11.9798	11.979	0.0634	0.0845	0.6877
Lena	12.0248	12.0248	0.0252	0.0482	0.6622
Devi	16.9614	16.9614	0.1374	0.0348	0.9796

The output of class-specific Richardson-Lucy is shown in Fig.10 which shows the test image, degraded, restored image, and corresponding 2D FFT. Also evaluated the performance metrics of Caltech 101-5 dataset and Dataset-2 and tabulated the outcomes are displayed in Table 6 and Table 8.

5 Conclusion

We have successfully experimented with and generated degraded images from different standard benchmark images. Using these degraded images, we restored the original image using the standard Richardson-Lucy deconvolution algorithm. We also observed the visual effect of different noises on images. The amount of degradation with respect to different types of noises and associated parameters was also analyzed. We observed

the performance metrics for some standard images. Determined the MSE, PSNR, SSIM, and KL Divergence. Evaluated the performance metrics for different cases by setting PSF kernel sizes of 5x5, 10x10, and 20x20 pixels. Experimented with the standard Richardson-Lucy deconvolution algorithm, modified Richardson-Lucy deconvolution algorithm, and class-specific Richardson-Lucy deconvolution algorithm. Restored the image using these three methods and evaluated the performance metrics. It is observed that the class-specific Richardson-Lucy deconvolution algorithm shows better performance than other methods.



(a) Test image (d) 2DFFT of the test image

(b) Degraded image (e) 2DFFT of Degraded image

(c) Restored image (f) 2DFFT of Restored image

Fig 10. Representative test degraded and restored images and their corresponding 2DFFT for the Class-specific Richardson-Lucy deconvolution method.

Conflict of Interest

The authors declare no conflict of interest of any kind such as financial, commercial or other relationship that might be perceived as representing a potential conflict of interest by the academic community:

Author Contributions

The conceptualization of the methodologies adopted in this paper has been done by JS and SM. SM created the methodology and the pipeline for experimentation. All experimentations were performed by JS and observations were compiled and scrutinized by AM. The original manuscript was prepared by JS and proof reading and thorough corrections were done by SM.

Funding

The authors declare that there is no funding received from any private, public and Government organization for conducting the research involved in the preparation of this paper.

Informed Consent Statement

This research does not include any experiments involving human. Hence informed consent statement is not applicable.

Declaration of generative AI and AI-assisted technologies

The authors declare that no generative AI or AI-assisted technologies were used in the writing process of this manuscript.

Acknowledgment

The authors wish to thank Dr. Agnes Jacob, HOD, for extending the laboratory facilities of Applied Electronics and Instrumentation Engineering department, Government Engineering College Kozhikode, Kerala, India for conducting the necessary experiments associated with this paper.

Appendix

Appendices, if needed, appear before the acknowledgment.

References

[1] C.H. Chen and XianjuWang "ANovel Theory of SARImage Restoration and Enhancement with ICA," ECE Dept., University of Massachusetts Dartmouth, N. Dartmouth, MA 02747 USA.

[2] Yibao Li, Qing Xia, Chaeyoung Lee, Sangkwon Kim, Junseok Kim "A robust and efficient fingerprint image restoration method based on a phase-field model," School of Mathematics and Statistics, Xi'an Jiaotong University, Xi'an, China.

[3] Francisco J. Gonzalez-Serrano, Harold. I: Molina-Bulla and Juan J. Murillo-Fuentes "Independent Component Analysis applied to Digital Image Watermarking," Universidad Carlos 111, DTC, ATSC, Butarque, 15, 2891 1 Leganks, Madrid, Spain.

[4] Franziska Schirrmacher, Christian Riess, and Thomas Kohler, "Adaptive Quantile Sparse Image (AQuaSI) Prior for Inverse Imaging Problems," IEEE Transaction on Computational Imaging, Vol. 6, 2020.

In Press

[5] Guoqing Wang, Changming Sun, and Arcot Sowmya, "Attentive Feature Refinement Network for Single Rainy Image Restoration," IEEE Transaction on Image Processing, Vol. 30, 2021.

[6] Santiago Lopez-Tapia, Rafeal Molina, Aggelos K. Katsggelos "Deep learning approaches to inverse problems in imaging: Past, present and future," Department of Computer Science and Artificial Intelligence, University of Granada, Spain.

[7] Wei Wang, Fang Li, and Michael K. Ng, "Structural Similarity-Based Nonlocal Variational Models for Image Restoration," IEEE Transaction on Image Processing, Vol. 28, no. 9, 2019.

[8] Isfaq Basir, Adil Majeed, Owais Khursheed, "Image Restoration and the various Restoration Techniques used in the field of Digital Image Processing," International Journal of Computer Science and Mobile Computing, Vol.6, Issue.6, 2017.

[9] Gopal Harikumar, Yoram Bresler, "Perfect Blind Restoration of Images Blurred by Multiple Filters: Theory and Efficient Algorithms," IEEE Transaction on Image Processing, Vol. 8, no.2, 1999.

[10] Zhang, Mingli, and Christian Desrosiers. "High-quality image restoration using low-rank patch regularization and global structure sparsity." IEEE Transactions on Image Processing 28.2 (2018): 868-879.

[11] Gayatri, Mirajkar. "A semi-blind approach to deconvolution of motion blurred images using sub-band decomposition and independent component analysis." 2012 IEEE International Conference on Signal Processing, Communication and Computing (ICSPCC 2012). IEEE, 2012.

[12] Lehr, J., J-B. Sibarita, and J-M. Chassery. "Image restoration in X-ray microscopy: PSF determination and biological applications." IEEE transactions on image processing 7.2 (1998): 258-263.

[13] Bioucas-Dias, José M., and Mário AT Figueiredo. "A new TwIST: Two-step iterative shrinkage/thresholding algorithms for image restoration." IEEE Transactions on Image processing 16.12 (2007): pp 2992-3004.

[14] Bonmassar, Giorgio, and Eric L. Schwartz. "Real-time restoration of images degraded by uniform motion blur in foveal active vision systems." IEEE Transactions on Image Processing 8.12 (1999): pp 1838-1842.

[15] Chen, Yong, et al. "Hyperspectral image restoration using weighted group sparsity-regularized low-rank tensor decomposition." IEEE Transactions on Cybernetics 50.8 (2019): pp 3556-3570.

[16] Guerrero-Colón, Jose A., Luis Mancera, and Javier Portilla. "Image restoration using space-variant Gaussian scale mixtures in overcomplete pyramids." IEEE Transactions on Image Processing 17.1 (2007): pp 27-41.

[17] L. Qi et al., "Photoacoustic Tomography Image Restoration With Measured Spatially Variant Point Spread Functions," in IEEE Transactions on Medical Imaging, vol. 40, no. 9, pp. 2318-2328, Sept. 2021, doi: 10.1109/TMI.2021.3077022.

[18] W. Xu, X. Chen, H. Guo, X. Huang and W. Liu, "Unsupervised Image Restoration With Quality-Task-Perception Loss," in IEEE Transactions on Circuits and Systems for Video Technology, vol. 32, no. 9, pp. 5736-5747, Sept. 2022, doi: 10.1109/TCSVT.2022.3153685.

[19] Z. Liang, W. Zhang, R. Ruan, P. Zhuang and C. Li, "GIFM: An Image Restoration Method With Generalized Image Formation Model for Poor Visible Conditions," in IEEE Transactions on Geoscience and Remote Sensing, vol. 60, pp. 1-16, 2022, Art no. 4110616, doi: 10.1109/TGRS.2022.3227548.

[20] S. Jiang, J. Hu, X. Zhi, W. Zhang, D. Wang and X. Sun, "Local Adaptive Prior-Based Image Restoration Method for Space Diffraction Imaging Systems," in IEEE Transactions on Geoscience and Remote Sensing, vol. 61, pp. 1-10, 2023, Art no. 5601610, doi: 10.1109/TGRS.2023.3236767.

[21] S. Welker, H. N. Chapman and T. Gerkmann, "DriftRec: Adapting Diffusion Models to Blind JPEG Restoration," in IEEE Transactions on Image Processing, vol. 33, pp. 2795-2807, 2024, doi: 10.1109/TIP.2024.3383776.

[22] J. Jiang, Z. Zuo, G. Wu, K. Jiang and X. Liu, "A Survey on All-in-One Image Restoration: Taxonomy, Evaluation and Future Trends," in IEEE Transactions on Pattern Analysis and Machine Intelligence, vol. 47, no. 12, pp. 11892-11911, Dec. 2025, doi: 10.1109/TPAMI.2025.3598132.

[23] R. K. Cho, K. Sood and C. S. C. Channapragada, "Image Repair and Restoration Using Deep Learning," 2022 4th International Conference on Artificial Intelligence and Speech Technology (AIST), Delhi, India, 2022, pp. 1-8, doi: 10.1109/AIST55798.2022.10065203.

[24] H. Gao and D. Dang, "Exploring Richer and More Accurate Information via Frequency Selection for Image Restoration," in IEEE Transactions on Circuits and Systems for Video Technology, vol. 35, no. 3, pp. 2689-2700, March 2025, doi: 10.1109/TCSVT.2024.3494239.

In Press

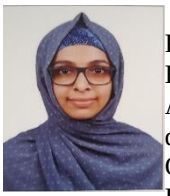
[25] B. L. Devi, Y. K. Chakravarti and B. V. Vinutna, "Advanced Image Restoration for Visual Clarity Enhancement," 2024 OITS International Conference on Information Technology (OCIT), Vijayawada, India, 2024, pp. 143-148, doi: 10.1109/OCIT65031.2024.00034.

[26] A. Mahapatra, M. A. Faruquee and P. Kumar, "Restoration of motion blurred image using Lucy Richardson Algorithm," 2018 International Conference on Communication, Computing and Internet of Things (IC3IoT), Chennai, India, 2018, pp. 73-76, doi: 10.1109/IC3IoT.2018.8668143.

Biographies (All Authors)



Dr. Shajee Mohan B S is currently working as a Professor in Computer Science and Engineering, SSET, Sharda University, India. Dr. Shajee Mohan obtained his Ph.D. from CSE Department, Indian Institute of Technology Madras, M.Tech from Visvesvaraya Technological University (VTU) and B.Tech from the University of Kerala. Before joining Sharda University, he served as professor and Dean (Research) at Government Engineering College Kozhikode, under the Directorate of Technical Education, Govt. of Kerala. He served over 30 years in various premier engineering institutes under Govt. of Kerala. He was the Head of CSE department, LBS College of Engineering Kasaragod, Govt. College of Engineering Kannur. He served as a member of BoS in Kannur, Calicut Universities in Kerala. He was also Chairman of BoE in Kannur, Calicut and APJ Abdul Kalam Technological Universities in Kerala. He has guided more than 25 M.Tech projects and at present guiding 3 Ph.D. research scholars under APJ KTU. He is a member of several Doctoral Committees (DC) and served as a thesis examiner for Kerala University and Anna University, Chennai. He is also a reviewer for several prestigious international journals including Expert Systems (Wiley), IEEE Access, Concurrency and Computation: Practice and Experience (Wiley), and Ecological Informatics (Elsevier). He also received several best paper awards at international conferences.



Jaliba Sherin Thottathil works as a Robotics Teacher at Mohammed Bin Hamad Al Sharqi School, Fujairah, United Arab Emirates. She holds an M.Tech degree in Signal Processing from Government Engineering College Kozhikode, Kerala, India, and a B.Tech degree in Electronics and Communication Engineering from Eranad Knowledge City Technical Campus, Malappuram, Kerala, India. Her master's research focused on optimizing the Richardson-Lucy Deconvolution Algorithm for image restoration. She has over two years of experience in teaching Robotics and STEM education. Prior to her current role, she served as a Robotics Teacher at Pace International School, Sharjah. She has guided students to achieve national-level accolades such as Young Scientists and Young Engineers through project-based learning and innovation. She has presented innovative student projects at national exhibitions conducted by the UAE Ministry of Education and has been recognized with awards such as the Conscientious Teacher Award and Certificate of Appreciation for excellence in mentoring. Her research interests include image and signal processing, computer vision, artificial intelligence, smart systems, and environmental sustainability.



Dr. Ahammed Muneer K V is currently working as Associate Professor in Electronics and Communication Engineering Department of Government Engineering College Kozhikode, Kerala, India. He completed B. Tech from College of Engineering Trivandrum, M. Tech from Indian Institute of Technology Madras and PhD from National Institute of Technology Calicut, India. He has more than 20 years of teaching experience in various Engineering colleges under the Directorate of Technical Education Kerala. He is the recipient of Prof. Achim Bopp Hardware Project Award-2012 from IIT Madras and bagged the best teacher award in 2022 under Indian Society for Technical Education (ISTE), Kerala Section. He had presented papers in international conferences at Penang, Malaysia and Valencia, Spain. He received several best paper awards and also delivered many invited talks and coordinated training for both students and faculties. He is a life member of ISTE, India and Senior member of IEEE. His research interest includes Biomedical signal and Image processing, Machine learning, Speech Processing, Smart Systems Design and Artificial Intelligence.

In Press